

# QoS-Aware Joint Power Allocation and Task Offloading in a MEC/NFV-enabled C-RAN Network

Mohsen Tajallifar, Sina Ebrahimi, Mohammad Reza Javan, Nader Mokari,  
and Luca Chiaraviglio,

## Abstract

In this paper, we propose a novel resource management scheme that jointly allocates the transmit power and network function virtualization (NFV) resources in a centralized radio access network (C-RAN) architecture consisting of several remote radio heads (RRHs) and a baseband unit (BBU) pool. The BBU pool is connected to a set of NFV-enabled nodes (including the multi-access\mobile edge computing (MEC)-enabled node) to which the requested tasks of user equipments (UEs) are offloaded. We formulate an optimization problem taking into account the transmission, execution, and propagation delays of each task with the aim to allocate the transmission power in radio and computational resources in nodes such that the user's maximum tolerable latency is satisfied. Since the proposed optimization problem is highly non-convex, we adopt the alternate search method (ASM) to achieve a sub-optimal solution. Moreover, a novel heuristic algorithm is proposed to jointly manage the allocated computational resources and placement of the tasks derived by ASM. We also propose a new admission control mechanism for finding the set of tasks that can be served by the available resources. Furthermore, a disjoint method that separately allocates the transmission power and the computational resources is proposed as the baseline of comparison. The simulation results show that the joint method outperforms the disjoint task offloading and power allocation. Specifically, for a specific setup, the joint method can provide 50 percent of acceptance ratio while the acceptance ratio of disjoint method is 25 percent when the maximum tolerable latency of tasks is equally divided between power allocation and task offloading steps. Moreover, with the proposed heuristic algorithm, the value of acceptance ratio is equal to 1 for

M. Tajallifar, S. Ebrahimi, and N. Mokari are with the Department of Electrical and Computer Engineering, Tarbiat Modares University, Tehran, 14115-111 Iran e-mail: nader.mokari@modares.ac.ir. M. Javan is with Shahrood University of Technology. L. Chiaraviglio is with University of Rome Tor Vergata.

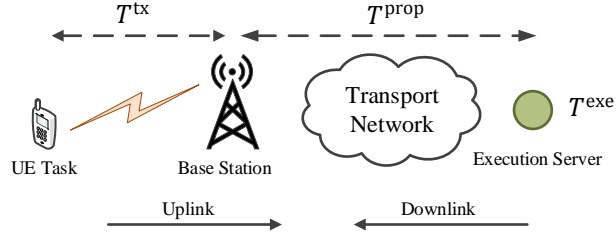


Fig. 1: A typical task offloading example

maximum tolerable latencies larger than 50 ms, while without heuristic algorithm, the acceptance ratio decreases to 65 percent.

### Index Terms

Multi-access\Mobile Edge Computing (MEC), Task Offloading, Network Function Virtualization (NFV), Admission Control, Centralized Radio Access Network (C-RAN).

## I. INTRODUCTION

In order to fulfill the requirements of 5G mobile networks, some enabling technologies such as network function virtualization (NFV) and multi-access\mobile edge computing (MEC) are introduced. With NFV, the network functions (NFs) that traditionally used dedicated hardware are implemented in applications running on top of commodity servers [1]. On the other hand, MEC aims to support low-latency mobile services by bringing the remote cloud servers closer to the mobile users [2], [3]. Moreover, MEC enables the offloading of the computational burden of users' tasks to reduce the impact of the limited battery power of user equipment (UE).

A typical task offloading example is shown in Fig. 1. The main idea of the task offloading is to transmit the non-processed data of a task from user equipment to an execution server that offloads the computational burden of the task execution on the remote server. As Fig. 1 shows, the user transmits the non-processed data of the task over the wireless link in the uplink to its serving base station. This task introduces transmission delay  $T^{tx}$ . Then, the received data should be transmitted to an execution server. Execution servers may be placed at any node in the network, i.e., ranging from the base station itself to a distant node in the core network. The data transmission through the transport network adds the propagation delay  $T^{prop}$  to the offloading process. Finally, the received data is processed at the execution server with delay  $T^{exe}$  and then is

transmitted back to the associated user over the downlink. Therefore, the overall task offloading latency is equal to the summation of all the above mentioned mentioned delays in both the uplink and the downlink directions.

#### A. Motivation

The task offloading methods proposed so far [4], [5] mainly consider only the task placement and computational resource allocation, ignoring the impact of the radio resource allocation. However, ignoring the radio access network is not only unrealistic but also makes the task offloading mechanism inefficient. Therefore, it is of mandatory importance to allocate the resources both in the radio access network and the MEC-enabled nodes which results in efficiency enhancement. With a joint task offloading and radio resource allocation, the shortcomings of one type of resources (i.e., computational or radio resources) can be compensated by the other type of resources, thus making possible to serve more tasks with lower total cost.

#### B. Contributions

In this paper, we consider an innovative task offloading problem, whose goal is to jointly optimize the computational and radio resource allocation. Specifically, a task is offloaded to an NFV-enabled node for execution and then the processed data of that task is forwarded through a network of NFV-enabled nodes towards a radio access network with centralized radio access network (C-RAN) architecture. The data, then, is transmitted to the intended user through a wireless link. In contrast to many works in the literature that consider the task offloading to a set of specific MEC-enabled nodes [6]–[8], we consider that the tasks can be offloaded to any node in the network as long as their requirements are fulfilled. Moreover, many works try to minimize the delay in task offloading. However, a typical task is required to be executed in a specific time duration. Consequently, the violation of experienced latency of task offloading from a minimum value results in performance degradation. Therefore, we aim to offload the tasks under a maximum tolerable latency constraint. Furthermore, in contrast to many works that consider a set of feasible task requests [8], [9], we propose an admission control mechanism that tries to find a subset of feasible tasks with maximum cardinality. The main contributions of this paper are summarized as follows:

- **Joint power allocation and task offloading (JPATO):** In this paper, we model both radio transmission power allocation and task offloading in a C-RAN architecture empowered by

NFV-enabled nodes. These NFV-enabled nodes can be located either at the edge of the radio network or in other places at a large distance from the radio network. We model end to end (E2E) latency of tasks as the summation of radio transmission, propagation through transport network, and processing delays. We further assume that each task should be served under a maximum tolerable E2E latency constraint. We also model the cost of serving tasks as the composition of the following terms: i) radio power consumption, ii) forwarding through transport network links, and iii) consumed power at NFV-enabled nodes. Therefore, the overall objective is to serve the requested tasks under latency constraints while ensuring the minimum cost.

- **Admission control:** As serving of all the incoming requests may not be feasible, we adopt an admission control mechanism, whose aim is to find the maximum cardinality subset of tasks that can be served by available resources in the network. In doing so, we propose to elasticize the constraints of the optimization problem by non-negative auxiliary variables (which we denote as "elastic variables"). The elastic variables take the zero value for feasible problem. Otherwise, they assume positive value in the case of infeasibility. Thus, we eliminate the tasks with associated positive elastic variables one by one, until a subset of feasible tasks is obtained.
- **Solution:** Since both JPATO and the admission control optimization problems are non-convex, we adopt an alternate search method (ASM) to find a sub-optimal solution by solving optimization subproblems with respect to each optimization variable. Furthermore, we adopt the convex-concave procedure (CCP) to overcome the non-convexity of the power allocation subproblem. Moreover, the task offloading subproblem is reformulated as an integer linear programming (ILP). Eventually, we propose a new heuristic algorithm in order to improve the performance of ASM in the proposed admission control algorithm.
- **Disjoint optimization:** We further provide a disjoint algorithm for radio transmission power allocation and task offloading as the baseline of comparison. In doing so, we decouple the maximum tolerable E2E latency of tasks into two parts: radio transmission and task offloading. We first consider the subproblem of radio transmission power allocation under its latency constraint which albeit includes an admission control mechanism. Then, the task offloading subproblem is solved under its associated latency constraint that again includes an admission control mechanism.
- **Convergence:** The convergence of both admission control and JPATO optimization algo-

rithms is proved by showing that the objective function values of the optimization subproblems are non-increasing in each iteration.

- **Complexity:** We analyze the computational complexity of the proposed algorithms including the interior-point method (IPM) and the proposed heuristic algorithm.

### C. Organization

The rest of this paper is organized as follows. Section II summarizes the related works in the task offloading literature. Section III introduces the system model. Section IV describes the optimization problem formulation. In Section V, we propose JPATO algorithm as well as the admission control mechanism, while the disjoint power allocation and task offloading (DPATO) algorithm is proposed in Section VI. The computational complexity analysis of the proposed methods is provided in Section VII. The simulation results are presented in Section VIII. Finally, we conclude the paper in Section IX.

### D. Notation

The notation used in this paper are given as follows. The vectors are denoted by bold lowercase symbols. Operators  $\|\cdot\|$  and  $|\cdot|$  are vector norm and absolute value of a scalar, respectively.  $(\mathbf{a})^T$  stands for transpose of  $\mathbf{a}$  and  $[a]^+ = \max(a, 0)$ .  $\mathcal{A} \setminus \{a\}$  discards the element  $a$  from the set  $\mathcal{A}$ . Finally,  $\mathbf{a} \sim \mathcal{CN}(\mathbf{0}, \Sigma)$  is a complex Gaussian vector with zero mean and covariance matrix  $\Sigma$ .

## II. RELATED WORKS

We classify the related works into five categories: Virtual Network Function (VNF) Placement [10], [11], task offloading in MEC [6], [7], [12], joint radio and computational RA [5], [8], [13]–[15], and admission control mechanisms [16], [17]. We will discuss each category briefly in the following.

1) **Virtual Network Function (VNF) Placement:** The authors in [10] thoroughly discuss advances and challenges about RA in NFV and have classified NFV-RA into three stages (i.e., VNFs chain composition, VNF forwarding graph embedding, and VNFs scheduling) in which VNF placement (VNF forwarding graph embedding) is the second stage of NFV-RA. The authors in [11] jointly allocate paths between nodes and place VNFs in an energy-efficient way, while the required latency and traffic rate of flows are guaranteed. In [16], the authors jointly solve the

problems of admission control and VNF placement. Moreover, [18] proposes and investigates solutions for the VNF placement and scheduling with the objective of minimizing the operator cost. In contrast to the classical VNF placement methods, wherein the impact of radio resources is ignored, in this paper, we propose to jointly optimize the task placement over the NFV-enabled nodes and radio resource allocation.

2) **Task Offloading in MEC:** Energy consumption minimization and latency satisfaction (or minimization) are two major goals of task offloading in MEC environment [2], [19]. A joint problem of task offloading and RA is solved by the authors of [12] in order to minimize the task completion time and user's energy consumption. The authors in [6] propose a greedy heuristic as a solution for the energy consumption minimization problem. In their solution, the maximum tolerable processing latency of the tasks is satisfied in a multiple MEC server environment. In [7] an energy-efficient offloading problem is solved with the objective to minimize the overall network energy cost and guarantee the latency requirements of UE's tasks in MEC. Furthermore, [20] considers only the radio resource allocation where the computational resources are neglected. In conventional MEC task offloading methods, the impact of radio resource allocation is neglected. On the contrary, we propose to jointly optimize the task offloading and radio resource allocation.

3) **Joint Radio and Computational Resource Allocation:** In [8], the authors provide a distributed algorithm to solve the joint task scheduling and resource allocation problem with the network power minimization objective. They offload the tasks in a way that the delay constraint is met in a downlink C-RAN architecture. A multi-user MEC computation offloading system is presented in [13], where the authors show that their solution reduces the sum cost of delay and energy consumption for all the end user devices. An allocation scheme of computation and radio resources in order to minimize the overall cost of computation, energy consumption, and maximum delay among users is presented in [14]. The authors in [5] model a MEC task offloading control problem considering a C-RAN environment composed of virtual machines (VMs). The authors solve the problem through three matching stages, namely between RRHs and UEs, BBUs and UEs, and VMs and UEs. Although the joint resource allocation is performed in some works, they suffer from some restrictive assumptions. For example, [8] and [13] offload all the tasks to one single node. However, when the maximum tolerable latency of some tasks is large, they can be offloaded in more distant nodes, leaving the computational resources of the edge node (e.g., BBU pool) free for the low latency tasks. Another restrictive assumption of the

existing works is that they mostly aim to minimize the latency of tasks without considering a maximum tolerable latency for each task [5], [14]. Therefore, in this paper, we propose a joint radio and computational resource allocation method which is able to offload the tasks to any node in the network as long as the corresponding maximum tolerable latency of each task is guaranteed.

4) **Admission Control Mechanisms:** Most of the existing works assume serving requested tasks with a given admission control without specifying how to obtain the set of feasible tasks. In [16], the authors investigate the admission control problem through defining an admission vector. The proposed admission control mechanism is applied to VNF requests. The problems of admission control, computational resource allocation, and power control in edge computing for Internet of Things are formulated in [17]. The authors consider their admission control mechanism for guaranteeing the QoS and the remaining network resources.

### III. SYSTEM MODEL

#### A. Radio Access Network

We consider a C-RAN architecture with a baseband unit (BBU) pool which serves a set of  $U$  radio remote heads (RRHs). Each RRH is equipped with  $M$  antennas. The set of all users is denoted by  $\mathcal{K}$ . The total number of users is  $K = |\mathcal{K}|$ , each of which is equipped with a single antenna. The considered model is shown in Fig. 2. It is assumed that each RRH is connected to the BBU pool through a fronthaul link.

We assume the each user requests a single task. Each UE task  $k$  is represented by a triplet  $\phi_k = \langle L_k, D_k, T_k \rangle$ , where  $L_k$  is the load of task  $k$  (i.e., the required CPU cycles),  $D_k$  is the data size of task  $k$  (in terms of bits), and  $T_k$  is the maximum tolerable latency of task  $k$ .

Each user transmits the data of the corresponding task to its serving RRH through a wireless link in the uplink direction. We assume that each user is served by a single RRH. The set of users served by RRH  $u$  is  $\mathcal{K}_u = \{k \in \mathcal{K} | J_u^k = 1\}$  where  $J_u^k$  is an indicator which equals 1 if user  $k$  is connected to RRH  $u$  (0 otherwise). In this paper, we assume that the user-RRH assignment is given and fixed. We assume a narrow-band block fading channel model. The channel vector between user  $k$  and RRH  $u$  is denoted by  $\mathbf{h}_{u,k}$ , where  $\mathbf{h}_{u,k} = \sqrt{Q_{u,k}} \tilde{\mathbf{h}}_{u,k}$  in which  $Q_{u,k}$  represents the path loss between RRH  $u$  and UE  $k$  and small-scale fading is modeled as  $\tilde{\mathbf{h}}_{u,k} \sim \mathcal{CN}(\mathbf{0}, \mathbf{I}_M)$ . The user  $k$  transmits a symbol  $x_k \sim \mathcal{CN}(0, 1)$  with transmit power  $\rho_k$  toward its serving RRH.

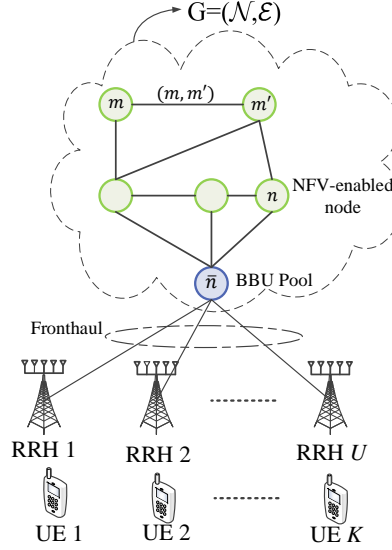


Fig. 2: The system model.

The transmit power of each user is constrained to a maximum value, i.e.,  $\rho_k \leq P_k^{\max} \quad \forall k$ . The following signal vector is received at the  $u^{\text{th}}$  RRH

$$\mathbf{y}_u = \sum_{k \in \mathcal{K}} \mathbf{h}_{u,k} \sqrt{\rho_k} x_k, \quad \forall u, \quad (1)$$

and is processed with the maximum ratio combining method. The combined signal is given by

$$\mathbf{z}_u = \mathbf{F}_u^H \mathbf{y}_u, \quad \forall u, \quad (2)$$

where  $\mathbf{F}_u = [\mathbf{f}_k]$ ,  $\forall k \in \mathcal{K}_u$  and  $\mathbf{f}_k = \frac{\mathbf{h}_{u,k}}{\|\mathbf{h}_{u,k}\|}$ . Therefore, the decision signal of user  $k$  is given by

$$z_k = \mathbf{f}_k^H \mathbf{h}_{u,k} \sqrt{\rho_k} x_k + \sum_{j \in \mathcal{K} \setminus \{k\}} \mathbf{f}_k^H \mathbf{h}_{u,j} \sqrt{\rho_j} x_j + \mathbf{f}_k^H \mathbf{n}_u, \quad \forall k \in \mathcal{K}_u,$$

where  $\mathbf{n}_u \sim \mathcal{CN}(\mathbf{0}, \sigma^2 \mathbf{I}_M)$  is the received noise vector at the  $u^{\text{th}}$  RRH. Thus, the signal to interference plus noise ratio (SINR) of user  $k$  can be written as

$$\text{SINR}_k = \frac{\|\mathbf{h}_{u,k}\|^2 \rho_k}{\sum_{j \in \mathcal{K} \setminus \{k\}} \frac{|\mathbf{h}_{u,k}^H \mathbf{h}_{u,j}|^2}{\|\mathbf{h}_{u,k}\|^2} \rho_j + \sigma^2}, \quad \forall k \in \mathcal{K}_u. \quad (3)$$

Hence, the achievable data rate for user  $k$  is  $R_k = W \log_2(1 + \text{SINR}_k)^1$  bits per second (bps), where  $W$  is the radio access network bandwidth. Therefore, the incurred delay related to task  $k$ 's data transmission of the uplink is given by  $T_k^{\text{tx}} = \frac{D_k}{R_k}$ .<sup>2</sup> Finally, the sum of data rates served

<sup>1</sup>For wide-band channel model, the data rate of user  $k$  is determined by the sum rate of all sub-carriers allocated to user  $k$ .

<sup>2</sup>It should be noted that no buffering is assumed in the transport network switching. Therefore, there is no need for transmission time of tasks traffic associated with the network graph links to be taken into account.



by RRH  $u$  should be less than the bandwidth of fronthaul links, i.e.,  $\sum_{k \in \mathcal{K}_u} R_k \leq B_{f,u}, \forall u$ .

In this paper, similar to [13], [21], [22], we assume the output data size of task  $k$  after the execution is small. Moreover, since the power budget in downlink direction is generally large, the transmission delay of downlink can be assumed negligible and therefore, our focus in the radio access network is solely on the uplink.

### B. NFV-enabled Network

The NFV-enabled nodes are interconnected through a network  $G = (\mathcal{N}, \mathcal{E})$  where  $\mathcal{N}$  and  $\mathcal{E}$  are the set of nodes and links connecting the nodes, respectively. A typical node in  $\mathcal{N}$  is denoted by  $n$  while the BBU pool is indicated by  $\bar{n}$  (which also is a node in  $\mathcal{N}$ ). Moreover, the link between two nodes  $m$  and  $m'$  is denoted by  $(m, m')$ . The nodes and links of the network can provide a limited amount of resources. The processing capacity (i.e., the maximum CPU cycles per second that could be carried out) of NFV-enabled node  $n$  is indicated by  $\Upsilon_n$ . Moreover, the bandwidth of link  $(m, m')$  is indicated by  $B_{(m, m')}$  in terms of bps.

A task offloading decision consists of specifying the placement of each task at node  $n$  and its associated path from  $\bar{n}$  to  $n$ . We denote the  $b^{\text{th}}$  path between nodes  $\bar{n}$  and  $n$  as  $p_n^b$  where  $b \in \mathcal{B}_n = \{1 \cdots B_n\}$  and  $B_n$  is the total number of paths between nodes  $\bar{n}$  and  $n$ . In order to choose a node and its associated path, we define the decision variable  $\xi_{p_n^b}^k$  which equals 1 when the task  $\phi_k$  is placed at node  $n$  and sent over path  $p_n^b$  and equals 0 otherwise. To ensure that a task is offloaded to one and only one node and path, we introduce the following constraint:

$$\sum_{n \in \mathcal{N}} \sum_{b \in \mathcal{B}_n} \xi_{p_n^b}^k = 1, \quad \forall k. \quad (4)$$

To determine whether a link contributes to a path, the indicator  $I_{p_n^b}^{(m, m')}$  is defined, which is equal to 1 when link  $(m, m')$  contributes to path  $p_n^b$  (0 otherwise). Moreover, the set of all links that contribute to a path can be defined as  $\mathcal{E}_{p_n^b} = \{(m, m') \in \mathcal{E} | I_{p_n^b}^{(m, m')} = 1\}$ . The amount of computational resources allocated to task  $k$  is denoted by  $v_k$  (in terms of CPU cycles per second). We assume that the execution of tasks are fully performed at only one node (i.e., full offloading). To ensure that the allocated computational resources do not violate the processing capacity of that node, we should have

$$\sum_{k \in \mathcal{K}} \sum_{b \in \mathcal{B}_n} v_k \xi_{p_n^b}^k \leq \Upsilon_n, \quad \forall n. \quad (5)$$

Since the data of task  $k$  is sent over the network with rate  $R_k$ , the aggregated rates of all tasks that pass a link should not exceed its bandwidth. This can be ensured by the following constraint:

$$\sum_{k \in \mathcal{K}} \sum_{n \in \mathcal{N}} \sum_{b \in \mathcal{B}_n} I_{p_n^b}^{(m, m')} \xi_{p_n^b}^k R_k \leq B_{(m, m')}, \quad \forall (m, m') \in \mathcal{E}. \quad (6)$$

The incurred delay caused by execution of task  $k$  is  $T_k^{\text{exe}} = \frac{L_k}{v_k}$ . The data of task  $k$  is sent to NFV-enabled node  $n$  over the uplink for execution. After the execution of the task, it should be sent toward the BBU pool (i.e., node  $\bar{n}$ ) over the downlink. In this paper, we assume the path of uplink and downlink are the same. Therefore, the overall propagation delay of task  $k$  over the path  $p_n^b$  is twice the propagation delay of path  $p_n^b$ . Thus, the propagation delay of task  $k$  is given by  $T_k^{\text{prop}} = 2 \sum_{n \in \mathcal{N}} \sum_{b \in \mathcal{B}_n} \sum_{(m, m') \in \mathcal{E}_{p_n^b}} \xi_{p_n^b}^k \delta_{(m, m')}$ , where  $\delta_{(m, m')}$  is the propagation delay of link  $(m, m')$ . We assume that the bandwidth consumption of links imposes a specific cost to operators, thus we need to calculate the overall traffic of users that pass through links and determine the cost of passing this traffic. The overall cost of bandwidth consumption is calculated as  $\beta = \sum_{k=1}^K \sum_{n \in \mathcal{N}} \sum_{b \in \mathcal{B}_n} \sum_{(m, m') \in \mathcal{E}_{p_n^b}} \xi_{p_n^b}^k \gamma_{(m, m')} R_k$ , where  $\gamma_{(m, m')}$  determines the cost of transmitting 1 bps traffic on link  $(m, m')$ . Table I summarizes the notation used in the paper.

#### IV. PROBLEM FORMULATION

In this section, we formulate JPATO problem. The overall objective is to offload and execute the tasks with acceptable E2E latency in a cost-efficient fashion. The overall cost of task offloading includes: 1) the radio transmission cost, which includes the power consumption of all RRHs, 2) the forwarding cost associated with the traffic injected in the network, and 3) the cost of consumed power of NFV-enabled nodes. Hence, the overall cost function can be stated as  $\Psi(\boldsymbol{\xi}, \mathbf{v}, \boldsymbol{\rho}) = \beta + \zeta \sum_{k \in \mathcal{K}} \rho_k + \eta \sum_{n \in \mathcal{N}} \sum_{k \in \mathcal{K}} \sum_{b \in \mathcal{B}_n} \Lambda_n \xi_{p_n^b}^k v_k^3$ , where  $\boldsymbol{\xi} = [\xi_{p_1^1}^1, \dots, \xi_{p_N^K}^K]^T$ ,  $\mathbf{v} = [v_1, \dots, v_K]^T$ , and  $\boldsymbol{\rho} = [\rho_1, \dots, \rho_K]^T$  are the vectors of all  $\xi_{p_n^b}^k$ ,  $v_k$ , and  $\rho_k$ , respectively, and  $\Lambda_n$  denotes the computational energy efficiency coefficient of node  $n$  [23]. Moreover,  $\zeta$  and  $\eta$  are weight factors.

TABLE I: Main Notation

Notation	Definition	Notation	Definition
$U, M, K$	Number of RRHs, antennas and users	$W$	Radio access network bandwidth
$\mathcal{K}, \mathcal{N}, \mathcal{E}$	Set of all users, nodes and links	$\mathcal{K}_u$	Set of users served by RRH $u$
$\phi_k$	Task of UE $k$	$\mathbf{h}_{u,k}$	Channel vector between user $k$ and RRH $u$
$L_k, D_k, T_k$	Load, data size and maximum tolerable latency of task $k$	$\xi_{p_n^b}^k$	Decision variable for assignment of node $n$ and its associated path $p_n^b$ to task $\phi_k$
$\Upsilon_n$	Processing capacity of node $n$	$B_{f,u}$	Bandwidth of fronthaul link for RRH $u$
$B_{(m,m')}, \delta_{(m,m')}$	Bandwidth and propagation delay of link $(m, m')$	$\Lambda_n$	Computational energy efficiency coefficient of the node $n$
$\gamma_{(m,m')}$	Cost of forwarding traffic on $(m, m')$	$P_k^{\max}$	Power budget of user $k$
$p_n^b$	$b^{\text{th}}$ path between nodes $\bar{n}$ and $n$	$v_k$	Computational resources allocated to task $\phi_k$
$\mathcal{B}_n$	Set of paths between nodes $\bar{n}$ and $n$	$\rho_k$	Allocated transmission power to user $k$
$\mathcal{E}_{p_n^b}$	Set of all links that contribute in the path $p_n^b$	$\alpha_k$	Elasticization variable of task $\phi_k$
$I_{p_n^b}^{(m,m')}$	Indicator determining whether link $(m, m')$ contributes in path $p_n^b$	$R_k$	Data rate of task $k$
$J_u^k$	Indicator determining whether user $k$ is assigned to RRH $u$	$\tau_k^{\text{exe}}$	Execution delay of task $k$
$\tau_k^{\text{tx}}$	Radio transmission delay of task $k$	$\tau_k^{\text{prop}}$	Propagation delay of task $k$
$\beta$	Cost of bandwidth consumption		

Therefore, the joint power allocation and task offloading optimization problem can be written as

$$\begin{aligned}
& \min_{\xi, \mathbf{v}, \boldsymbol{\rho}} \Psi(\xi, \mathbf{v}, \boldsymbol{\rho}) \\
& \text{s.t.} \quad \text{C1: } T_k^{\text{exe}} + T_k^{\text{prop}} + T_k^{\text{tx}} \leq T_k, \quad \forall k, \\
& \quad \quad \text{C2: } \sum_{k \in \mathcal{K}} \sum_{b \in \mathcal{B}_n} v_k \xi_{p_n^b}^k \leq \Upsilon_n, \quad \forall n, \\
& \quad \quad \text{C3: } \sum_{k \in \mathcal{K}} \sum_{n \in \mathcal{N}} \sum_{b \in \mathcal{B}_n} I_{p_n^b}^{(m,m')} \xi_{p_n^b}^k R_k \leq B_{(m,m')}, \quad \forall (m, m') \in \mathcal{E}, \\
& \quad \quad \text{C4: } \sum_{k \in \mathcal{K}_u} R_k \leq B_{f,u}, \quad \forall u, \\
& \quad \quad \text{C5: } \rho_k \leq P_k^{\max}, \quad \forall k, \\
& \quad \quad \text{C6: } \sum_{n \in \mathcal{N}} \sum_{b \in \mathcal{B}_n} \xi_{p_n^b}^k = 1, \quad \forall k,
\end{aligned} \tag{7}$$

under variables:  $\xi \in \{0, 1\}$ ,  $\mathbf{v} \geq 0$ ,  $\boldsymbol{\rho} \geq 0$ . Constraint C1 guarantees that the maximum tolerable latency of task offloading is respected. Constraints C2 and C3 make sure that all tasks are offloaded without violation in computational capacity of nodes as well as bandwidth of links, respectively. Constraint C4 ensures the maximum capacity of fronthaul links. Constraint C5 corresponds to power budget of users while constraint C6 ensures that each task is offloaded at only one node and traversing only one path.

## V. JOINT POWER ALLOCATION AND TASK OFFLOADING (JPATO)

In this section, we propose a solution for optimization problem (7). This problem is highly non-convex due to the integer variable  $\xi$  as well as non-convexity of C1-C4. Therefore, we adopt an alternate search method (ASM) to divide the main problem into multiple subproblems, each of them associated to a proper subset of the optimization variable. Then, each set of variables is optimized given the values of other sets of variables and a sub-optimal solution can be obtained by the proposed iterative solution algorithm. The proposed ASM needs a feasible initialization. It is likely for constraint C1 to make the main problem infeasible. Thus, we need to propose an admission control mechanism to find the tasks that cause infeasibility. In the following, we exclude such tasks and we seek for the optimal solution of joint resource allocation problem for the remaining ones.

### A. Admission Control

To find the tasks which cause infeasibility, we use the elasticization approach of [24]. In particular, the constraints are elasticized by introducing elastic variables that extend the bounds on constraints. More formally, an infeasible set of constraints  $f_k(x) \leq 0$ ,  $k = 1, \dots, K$  can be elasticized by non-negative elastic variables  $\alpha_k$  as  $f_k(x) - \alpha_k \leq 0$ . A feasibility problem is then constructed by replacing the original objective function with the sum of elastic variables, i.e.,  $\sum_{k=1}^K \alpha_k$ , subject to elasticized constraints. By solving the feasibility problem, the constraints which cause infeasibility can be found by determining the constraints with positive associated elastic variables. The feasibility problem of (7) w.r.t. the optimization variables  $\xi, \mathbf{v}, \boldsymbol{\rho}$ , and  $\boldsymbol{\alpha}$  can be written as

$$\begin{aligned} & \min_{\xi, \mathbf{v}, \boldsymbol{\rho}, \boldsymbol{\alpha}} \quad \sum_{k \in \mathcal{K}} \alpha_k \\ & \text{s.t.} \quad \text{C1-a:} \quad T_k^{\text{exe}} + T_k^{\text{prop}} + T_k^{\text{tx}} - \alpha_k \leq T_k, \quad \forall k \in \mathcal{K} \\ & \quad \quad \text{C2-C6,} \end{aligned} \tag{8}$$

under variables:  $\xi \in \{0, 1\}$ ,  $\mathbf{v} \geq 0$ ,  $\boldsymbol{\rho} \geq 0$ ,  $\boldsymbol{\alpha} \geq 0$ . Note that only C1 of (8) is elasticized because by elimination of C1, the optimization problem (7) is always feasible. Thus, we seek for the tasks whose maximum tolerable latency is violated and eliminate them one by one until a feasible set of tasks remains. The solution of (8) not only provides the infeasible constraints but also determines the level of infeasibility, i.e., constraints with larger associated elastic variable need more resources to become feasible. Therefore, we start by eliminating of tasks with larger values of elastic variables.

Without loss of equivalence, we can add the summation of inequalities in C1-a as a new constraint to optimization problem (8). Therefore, the optimization problem (8) can be restated as

$$\begin{aligned}
& \min_{\xi, \mathbf{v}, \boldsymbol{\rho}, \boldsymbol{\alpha}} \sum_{k \in \mathcal{K}} \alpha_k \\
& \text{s.t.} \quad \text{C1-a: } T_k^{\text{exe}} + T_k^{\text{PROP}} + T_k^{\text{tx}} - \alpha_k \leq T_k, \quad \forall k \\
& \quad \text{C2-C6,} \\
& \quad \text{C7: } \sum_{k \in \mathcal{K}} (T_k^{\text{exe}} + T_k^{\text{PROP}} + T_k^{\text{tx}} - T_k) \leq \sum_{k \in \mathcal{K}} \alpha_k.
\end{aligned} \tag{9}$$

This optimization problem is equivalent of

$$\begin{aligned}
& \min_{\xi, \mathbf{v}, \boldsymbol{\rho}, \boldsymbol{\alpha}} \sum_{k \in \mathcal{K}} (T_k^{\text{exe}} + T_k^{\text{PROP}} + T_k^{\text{tx}}) \\
& \text{s.t.} \quad \text{C1-a, C2-C6,}
\end{aligned} \tag{10}$$

in which the term  $\sum_{k \in \mathcal{K}} T_k$  is removed from the objective due to its constant value. Therefore, given a random but feasible set of values for the discrete variable  $\xi$ , and a feasible power allocation complying with constraints C3 - C6, we first solve the feasibility problem (10) for  $\mathbf{v}$  and  $\boldsymbol{\rho}$ , respectively. The optimization problems associated with  $\mathbf{v} \geq 0$  and  $\boldsymbol{\rho} \geq 0$  can be respectively written as

$$\begin{aligned}
& \min_{\mathbf{v}} \sum_{k \in \mathcal{K}} T_k^{\text{exe}} \\
& \text{s.t.} \quad \text{C1-a, C2,}
\end{aligned} \tag{11}$$

and

$$\begin{aligned}
& \min_{\boldsymbol{\rho}} \sum_{k=1}^K T_k^{\text{tx}} \\
& \text{s.t.} \quad \text{C1-a, C3-C5.}
\end{aligned} \tag{12}$$

Since the function  $\frac{L_k}{v_k}$  is convex over  $v_k > 0$ , the subproblem (11) is convex and can be efficiently solved using Interior Point Method (IPM).

Given the optimal  $\mathbf{v}$  as the solution of (11), we solve (12) for  $\boldsymbol{\rho}$ . The objective function of (12) as well as the constraints C1-a, C3 and C4 are all non-convex. Therefore, we need to find a convexified version of this problem. We use the well-known convex-concave procedure [25] to convexify the objective function of (12) as follows:

$$R_k = W \log_2 \left( \frac{\sum_{j \in \mathcal{K}} \frac{|\mathbf{h}_{u,k}^H \mathbf{h}_{u,j}|^2}{|\mathbf{h}_{u,j}|^2} \rho_j + \sigma^2}{\sum_{j \in \mathcal{K} \setminus \{k\}} \frac{|\mathbf{h}_{u,k}^H \mathbf{h}_{u,j}|^2}{|\mathbf{h}_{u,j}|^2} \rho_j + \sigma^2} \right), \quad k \in \mathcal{K}_u, \tag{13}$$

hence

$$R_k = W \log_2 \underbrace{\left( \sum_{u=1}^U \sum_{j \in \mathcal{K}_u} \frac{|\mathbf{h}_{u,k}^H \mathbf{h}_{u,j}|^2}{|\mathbf{h}_{u,j}|^2} \rho_j + \sigma^2 \right)}_{h_k(\boldsymbol{\rho})} - W \log_2 \underbrace{\left( \sum_{u=1}^U \sum_{j \in \mathcal{K}_u \setminus \{k\}} \frac{|\mathbf{h}_{u,k}^H \mathbf{h}_{u,j}|^2}{|\mathbf{h}_{u,j}|^2} \rho_j + \sigma^2 \right)}_{g_k(\boldsymbol{\rho})}. \tag{14}$$

Each term of the objective function can be written as  $T_k^{\text{tx}}(\boldsymbol{\rho}) = \frac{D_k}{R_k} = \frac{D_k}{h_k(\boldsymbol{\rho}) - g_k(\boldsymbol{\rho})}$ . We leverage the first order of Taylor series in the vicinity of a given power allocation  $\boldsymbol{\rho}^0$  as  $\hat{T}_k^{\text{tx}}(\boldsymbol{\rho}) = T_k^{\text{tx}}(\boldsymbol{\rho}^0) + \nabla T_k^{\text{tx}}(\boldsymbol{\rho}^0)^{\text{T}}(\boldsymbol{\rho} - \boldsymbol{\rho}^0)$ , where  $\nabla T_k^{\text{tx}}(\boldsymbol{\rho}) = \frac{-D_k}{R_k^2}(\nabla h_k(\boldsymbol{\rho}) - \nabla g_k(\boldsymbol{\rho}))^3$ , in which

$$[\nabla h_k(\boldsymbol{\rho})]_i = \frac{W \sum_{u=1}^U I_u^i \frac{|\mathbf{h}_{u,k}^{\text{H}} \mathbf{h}_{u,i}|^2}{|\mathbf{h}_{u,i}|^2}}{\ln(2) \left( \sum_{u=1}^U \sum_{j \in \mathcal{K}_u} \frac{|\mathbf{h}_{u,k}^{\text{H}} \mathbf{h}_{u,j}|^2}{|\mathbf{h}_{u,j}|^2} \rho_j + \sigma^2 \right)}, \quad i \in \mathcal{K}, \quad (15)$$

and

$$[\nabla g_k(\boldsymbol{\rho})]_i = \begin{cases} \frac{W \sum_{u=1}^U I_u^i \frac{|\mathbf{h}_{u,k}^{\text{H}} \mathbf{h}_{u,i}|^2}{|\mathbf{h}_{u,i}|^2}}{\ln(2) \left( \sum_{u=1}^U \sum_{j \in \mathcal{K}_u \setminus \{k\}} \frac{|\mathbf{h}_{u,k}^{\text{H}} \mathbf{h}_{u,j}|^2}{|\mathbf{h}_{u,j}|^2} \rho_j + \sigma^2 \right)}, & i \in \mathcal{K} \setminus \{k\}, \\ 0, & i = k. \end{cases} \quad (16)$$

In order to find a convex approximation of C1-a in subproblem (12), we first reformulate it as  $T_k^{\text{exe},i} + T_k^{\text{prop},i} + \frac{D_k}{R_k} - \alpha_k \leq T_k$ , where  $T_k^{\text{exe},i}$  and  $T_k^{\text{prop},i}$  are the execution time and propagation time of task  $k$  obtained from the results of the subproblems associated with variables  $\mathbf{v}$  and  $\boldsymbol{\xi}$  at  $i^{\text{th}}$  iteration, respectively. Hence

$$R_k \geq \frac{D_k}{T_k + \alpha_k - T_k^{\text{prop},i} - T_k^{\text{exe},i}}. \quad (17)$$

In order to convexify (17), we need a concave approximation of  $R_k$  with respect to  $\boldsymbol{\rho}$ . Based on convex-concave procedure (CCP) [25], since both  $h_k(\boldsymbol{\rho})$  and  $g_k(\boldsymbol{\rho})$  are concave functions of  $\boldsymbol{\rho}$ , we need to find the linear approximation of  $g_k(\boldsymbol{\rho})$ . The linear approximation of  $R_k$  can be given as  $\hat{g}_k(\boldsymbol{\rho}) = g_k(\boldsymbol{\rho}^0) + \nabla g_k(\boldsymbol{\rho}^0)^{\text{T}}(\boldsymbol{\rho} - \boldsymbol{\rho}^0)$ .

In the following, we focus on the convex approximation of constraints C3 and C4. To this aim, we find a convex approximation of  $R_k$ . Again, based on CCP,  $h_k(\boldsymbol{\rho})$  should be approximated by a linear function. Thus, we have  $\hat{h}_k(\boldsymbol{\rho}) = h_k(\boldsymbol{\rho}^0) + \nabla h_k(\boldsymbol{\rho}^0)^{\text{T}}(\boldsymbol{\rho} - \boldsymbol{\rho}^0)$ . Now, the convexified version of subproblem (12) can be stated as

$$\begin{aligned} & \min_{\boldsymbol{\rho}} \quad \sum_{k \in \mathcal{K}} \nabla T_k^{\text{tx}}(\boldsymbol{\rho}^0)^{\text{T}}(\boldsymbol{\rho} - \boldsymbol{\rho}^0) \\ \text{s.t.} \quad & \text{C1-b} \quad h_k(\boldsymbol{\rho}) - \hat{g}_k(\boldsymbol{\rho}) \geq \frac{D_k}{T_k + \alpha_k - T_k^{\text{prop},i} - T_k^{\text{exe},i}}, \quad \forall k \in \mathcal{K} \\ & \text{C3-a:} \quad \sum_{k \in \mathcal{K}} \sum_{n \in \mathcal{N}} \sum_{b \in \mathcal{B}_n} I_{p_n^b}^{(m,m')} \xi_{p_n^b}^k \left( \hat{h}_k(\boldsymbol{\rho}) - g_k(\boldsymbol{\rho}) \right) \leq B_{(m,m')}, \quad \forall (m, m') \in \mathcal{E} \\ & \text{C4-a:} \quad \sum_{k \in \mathcal{K}_u} \left( \hat{h}_k(\boldsymbol{\rho}) - g_k(\boldsymbol{\rho}) \right) \leq B_{f,u}, \quad \forall u \\ & \text{C5:} \quad \rho_k \leq P_k^{\text{max}}, \quad \forall k, \end{aligned} \quad (18)$$

<sup>3</sup>The term  $R_k^2$  appears at the denominator due to the first order derivative of fractional functions.

under variable:  $\rho \geq 0$ . Starting from a feasible  $\rho^0$ , an iterative solution of (18) provides a sub-optimal solution of (12). The algorithm of CCP is shown in Algorithm 1. Now, given the

---

**Algorithm 1:** Convex-concave procedure for solving (12)

---

**Input:** Feasible  $\rho^0$ ,  $i = 0$ ,  $\epsilon = 10^{-3}$ ,  $I_{\max}^\rho = 10^3$

1 **repeat**

    % Allocate power to users

2     Solve (18) and set  $\rho^{i+1} = \rho^*$

3      $i = i + 1$

4 **until**  $\sum_{k \in \mathcal{K}} \hat{T}_k^{\text{tx}}(\rho^i) - \sum_{k \in \mathcal{K}} \hat{T}_k^{\text{tx}}(\rho^{i-1}) \leq \epsilon$  or  $i \geq I_{\max}^\rho$

**Output:**  $\rho^*$

---

solution of subproblems (11) and (18), we aim to find the binary decision variable  $\xi$ . The associated subproblem is

$$\begin{aligned} \min_{\xi} \quad & \sum_{k \in \mathcal{K}} T_k^{\text{prop}} \\ \text{s.t.} \quad & \text{C2, C3, C6.} \end{aligned} \quad (19)$$

This subproblem is an ILP problem and efficiently can be solved by MOSEK solver [26]. Finally, given  $\mathbf{v}$ ,  $\rho$ , and  $\xi$  as the solutions of the associated subproblems, the subproblem for finding elastic variable  $\alpha$  is given by

$$\begin{aligned} \min_{\alpha} \quad & \sum_{k \in \mathcal{K}} \alpha_k \\ \text{s.t.} \quad & \text{C1-a,} \end{aligned} \quad (20)$$

which is a linear programming and the solution is simply can be found as  $\alpha_k = [T_k^{\text{exe}} + T_k^{\text{prop}} + T_k^{\text{tx}} - T_k]^+$ . Since the objective of (19) is to minimize  $\sum_{k \in \mathcal{K}} T_k^{\text{prop}}$ , the solver tries to find the nodes with lowest associated propagation delay even if there are unused computational resources that can decrease the value of  $\sum_{k \in \mathcal{K}} (T_k^{\text{exe}} + T_k^{\text{prop}})$ . To resolve this issue, we consider the optimization problem

$$\begin{aligned} \min_{\alpha, \mathbf{v}, \xi} \quad & \sum_{k \in \mathcal{K}} \alpha_k \\ \text{s.t.} \quad & \text{C1-C3, C6,} \end{aligned} \quad (21)$$

which can offload the tasks to the nodes that can minimize  $T_k^{\text{exe}} + T_k^{\text{prop}}$ . In order to solve (21), we propose a novel heuristic method, whose goal is to search among all the nodes that can provide more computational resources to task  $\phi_k$ . To do so, we start from the tasks with the lowest positive values of elastic variable and calculate the amount of unused computational resources at all nodes which is given by  $\tilde{\Upsilon}_n^k = \Upsilon_n - \sum_{j \in \mathcal{K} \setminus \{k\}} \sum_{b \in \mathcal{B}_n} v_j \xi_{p_n^b}^j$ . Assuming

$v_k = \tilde{\Upsilon}_n^k$ , the value of  $T_k^{\text{exe}} + T_k^{\text{prop}}$  is calculated for all nodes which their paths have enough bandwidth. The available bandwidth of link  $(m, m')$  can be obtained as  $\tilde{B}_{(m, m')}^k = B_{(m, m')} - \sum_{j \in \mathcal{K} \setminus \{k\}} \sum_{n \in \mathcal{N}} \sum_{b \in \mathcal{B}_n} I_{p_n^b}^{(m, m')} \xi_{p_n^b}^j R_j$ . Then, having the available resources of nodes and links, the feasible node and path that minimize the value of  $T_k^{\text{exe}} + T_k^{\text{prop}}$  are selected. After that, we calculate the value of  $\tilde{\alpha}_k = T_k^{\text{exe}} + T_k^{\text{prop}} + T_k^{\text{tx}} - T_k$ . The negativeness of  $\tilde{\alpha}_k < 0$  means that task  $\phi_k$  is over-provisioned. Thus, we update  $v_k$  such that  $\tilde{\alpha}_k = 0$ . The ASM modification algorithm is provided by Algorithm 2. According to Algorithm 3, after the accomplishment of

---

**Algorithm 2:** ASM modification algorithm for solving (21)

---

**Input:**  $\alpha, \xi, v$

```

1 sort  $\alpha$ :  $\alpha_{[1]} \leq \alpha_{[2]} \leq \dots \alpha_{[|\mathcal{K}|]}$ 
2 for  $k = [1] : [|\mathcal{K}|]$  do
    % Find a feasible node according to the bandwidth of paths terminating at that node
3    $\mathcal{N}^k = \{n \in \mathcal{N} | \exists b : R_k \leq \tilde{B}_{(m, m')}^k \forall (m, m') \in \mathcal{E}_{p_n^b}\}$ 
4    $\tilde{\Upsilon}_n^k = \Upsilon_n - \sum_{j \in \mathcal{K} \setminus \{k\}} \sum_{b \in \mathcal{B}_n} v_j \xi_{p_n^b}^j, \quad \forall n$ 
    % Find the best node and associated path
5    $(n^*, b^*) = \arg \min_{n \in \mathcal{N}^k, b \in \mathcal{B}_n} T^{\text{exe}}(\tilde{\Upsilon}_n^k) + T^{\text{prop}}(\xi_{p_n^b}^k)$ 
    % Update elastic variables
6    $\tilde{\alpha}_k = T_k^{\text{tx}} + T_k^{\text{exe}}(\tilde{\Upsilon}_{n^*}^k) + T_k^{\text{prop}}(\xi_{p_{n^*}^{b^*}}^k) - T_k$ 
7   if  $\tilde{\alpha}_k < 0$  then
8     set  $v_k = \frac{L_k}{T_k - T_k^{\text{tx}} - T_k^{\text{prop}}}$ , and  $\alpha_k^* = 0$ 
9   else
10     $\alpha_k^* = \tilde{\alpha}_k$ 

```

**Output:**  $\alpha^*, \xi^*, v^*$

---

modified ASM, we find the value of the maximum elastic variable. If the maximum elastic value is positive, the associated task is rejected and the set of the served users is updated and then the feasibility problem is solved for the updated set of the served users. This procedure continues until there is no task with positive associated elastic variable. The output of the admission control algorithm is the set of feasible tasks  $\mathcal{K}^*$  as well as the solution of feasibility problem (8), i.e., the values of  $\xi^{\text{ini}}, \rho^{\text{ini}}$ , and  $v^{\text{ini}}$ , which are fed into the joint optimization algorithm for solving (7).



---

**Algorithm 3:** JPATO admission control algorithm for solving (8)

---

**Input:**  $\mathcal{K} = \{1, \dots, K\}$ ,  $i = 0$ ,  $\alpha^0 = \Theta$  (very large),  $\rho^0 = \epsilon$  (very small)

$\xi^0$ : random but compliant with C6

```

1 repeat
2   repeat
3     % Allocate the computational resources, power, and place the tasks, respectively
4     Solve (11) and set  $\mathbf{v}^{i+1} = \mathbf{v}^*$ 
5     Solve (12) via CCP in Algorithm 1 and set  $\rho^{i+1} = \rho^*$ 
6     Solve (19) and set  $\xi^{i+1} = \xi^*$ 
7     Update  $\mathbf{v}^{i+1}$ ,  $\xi^{i+1}$  and  $\alpha^{i+1}$  via Algorithm 2
8      $i = i + 1$ 
9   until  $\sum_{k \in \mathcal{K}} \alpha_k^{i-1} - \sum_{k \in \mathcal{K}} \alpha_k^i \leq \epsilon$  or  $i \geq I_{\max}$ 
10  % Eliminate the task with maximum associated elastic variable
11   $k^* = \arg \max_{k \in \mathcal{K}} \alpha_k$ 
12  if  $\alpha_{k^*} > 0$  then
13     $\mathcal{K} = \mathcal{K} \setminus \{k^*\}$ 
14  else
15    break
16 until  $\sum_{k \in \mathcal{K}} \alpha_k = 0$ 

```

**Output:**  $\xi^{\text{ini}}, \rho^{\text{ini}}, \mathbf{v}^{\text{ini}}, \mathcal{K}^*$

---

### B. Joint optimization

Given the solution of admission control problem  $\xi^{\text{ini}}, \rho^{\text{ini}}, \mathbf{v}^{\text{ini}}$ , and the set of accepted tasks  $\mathcal{K}$ , we seek for the solution of (7). Since the optimization problem (7) and the admission control problem (8) are very similar, the admission control algorithm is applicable to optimization problem with slight modifications. Again, we adopt the ASM for the solution of (7). The subproblems associated with each subset of variables are given in the following. The subproblem for obtaining computational resources is

$$\begin{aligned}
 & \min_{\mathbf{v}} \sum_{n \in \mathcal{N}} \sum_{k \in \mathcal{K}} \sum_{b \in \mathcal{B}_n} \Lambda_n \xi_{p_n^b}^k v_k^3 \\
 & \text{s.t.} \quad \text{C1, C2,}
 \end{aligned} \tag{22}$$

which is a convex optimization problem. The subproblem of power allocation, after convexification, is given by

$$\begin{aligned} \min_{\boldsymbol{\rho}} \quad & \sum_{k \in \mathcal{K}} \rho_k \\ \text{s.t.} \quad & \text{C1-c: } h_k(\boldsymbol{\rho}) - \hat{g}_k(\boldsymbol{\rho}) \geq \frac{D_k}{T_k - T_k^{\text{prop},i} - T_k^{\text{exe},i}}, \forall k \in \mathcal{K} \\ & \text{C3-a, C4-a, C5,} \end{aligned} \quad (23)$$

which can be solved using CCP. The task offloading subproblem can be written as

$$\begin{aligned} \min_{\boldsymbol{\xi}} \quad & \beta_c + \sum_{n \in \mathcal{N}} \sum_{k \in \mathcal{K}} \sum_{b \in \mathcal{B}_n} \Lambda_n \xi_{p_n^b}^k v_k^3 \\ \text{s.t.} \quad & \text{C1-C3, C6.} \end{aligned} \quad (24)$$

which is an ILP. It is important to note that the ASM modification approach is not leveraged for optimization algorithm because there is no motivation for placement of tasks to more distant nodes. This would result in an increase of the forwarding cost and therefore does not affect the computational cost. The optimization algorithm is provided in Algorithm 4.

---

**Algorithm 4:** JPATO optimization algorithm for solving (7) with admitted set of tasks

---

**Input:**  $\boldsymbol{\xi}^0 = \boldsymbol{\xi}^{\text{ini}}, \boldsymbol{\rho}^0 = \boldsymbol{\rho}^{\text{ini}}, \boldsymbol{v}^0 = \boldsymbol{v}^{\text{ini}}, \mathcal{K}^*, i = 0$

1 **repeat**

    % Allocate the computational resources, power, and place the tasks, respectively

2     Solve (22) and set  $\boldsymbol{v}^{i+1} = \boldsymbol{v}^*$

3     Solve (23) via CCP in Algorithm 1 and set  $\boldsymbol{\rho}^{i+1} = \boldsymbol{\rho}^*$

4     Solve (24) and set  $\boldsymbol{\xi}^{i+1} = \boldsymbol{\xi}^*$

5      $i = i + 1$

6 **until**  $\Psi(\boldsymbol{\xi}^{i-1}, \boldsymbol{v}^{i-1}, \boldsymbol{\rho}^{i-1}) - \Psi(\boldsymbol{\xi}^i, \boldsymbol{v}^i, \boldsymbol{\rho}^i) \leq \epsilon$  or  $i \geq I_{\text{max}}$

**Output:**  $\boldsymbol{\xi}^*, \boldsymbol{\rho}^*, \boldsymbol{v}^*$

---

### C. Convergence analysis

Now, we prove the convergence of the proposed admission control and the joint optimization methods for solving problems (8) and (7), respectively.

**Lemma 1.** *Algorithm 3 for solving problem (8) converges after sufficient number of iterations.*

*Proof.* In order to prove the convergence of Algorithm 3, it is sufficient to show that the value of objective function of problem (8), i.e.,  $\sum_{k \in \mathcal{K}} \alpha_k$  does not increase in any step of the algorithm.

It is obvious that the solutions of subproblems (11), (12), and (19) do not affect the value of the objective. However, as the objectives of these subproblems are to minimize the values of  $\sum_{k \in \mathcal{K}} T_k^{\text{exe}}$ ,  $\sum_{k \in \mathcal{K}} T_k^{\text{tx}}$ , and  $\sum_{k \in \mathcal{K}} T_k^{\text{prop}}$ , they extend the feasible set of subproblem (20) which results in reduction of  $\sum_{k \in \mathcal{K}} \alpha_k$ . Then, the optimization variables  $\mathbf{v}$  and  $\mathbf{e}$  are updated using the ASM modification algorithm. In line 5 of Algorithm 2, the value of  $T_k^{\text{exe}} + T_k^{\text{prop}}$  is minimized for each  $k$ , and hence, this value does not increase and so is for  $\tilde{\alpha}_k$  in line 6. On the other hand, it can be written that  $\alpha_k^* = [0, \tilde{\alpha}_k]^+$ , which is a non-decreasing function of  $\tilde{\alpha}_k$ . Therefore, the calculated  $\alpha_k^*$  does not increase in the ASM modification algorithm and the inequality  $\sum_{k \in \mathcal{K}} \alpha_k^{i+1} \leq \sum_{k \in \mathcal{K}} \alpha_k^i$  holds for each value of the iteration index  $i$ . Finally, since the value of the objective function is lower bounded by zero, the algorithm converges after sufficient number of iterations. After obtaining the solution of (8), the constraints associated with the task having the maximum elastic variable may be eliminated. This elimination is equivalent to removing the constraints of (8) associated with the eliminated task. Removing some constraints of (8) results in extension of the feasible set of (8) which in turn results in less objective value in the next iteration. Thus, the value of  $\sum_{k \in \mathcal{K}} \alpha_k$  is non-increasing in each step of the admission control algorithm and the algorithm finally converges to a sub-optimal solution.  $\square$

**Lemma 2.** *The Algorithm 4 of JPATO method converges after sufficient number of iterations.*

*Proof.* The joint optimization method in Algorithm 4 alternatively minimizes the objective function  $\Psi(\boldsymbol{\xi}, \mathbf{v}, \boldsymbol{\rho})$ . Therefore, the value of the objective function does not increase in each step of each iteration and converges after sufficient iterations. The convergence analysis of Algorithm 6 and Algorithm 7 involved in the disjoint method is similar to that of joint method algorithms (and it is omitted due to lack of space).  $\square$

#### D. Summary of the proposed method

Herein we summarize the proposed algorithms in previous subsections. Algorithm 5 provides a quick view of Algorithm 3 and Algorithm 4 for the proposed admission control and joint optimization methods, respectively.

## VI. DISJOINT POWER ALLOCATION AND TASK OFFLOADING (DPATO)

In order to better position the performance of the proposed JPATO algorithm, we introduce the Disjoint Power Allocation and Task Offloading (DPATO) as the baseline of comparison. In

---

**Algorithm 5:** Summary of Algorithms 3 and 4
 

---

**Input:**  $\mathcal{K} = \{1, \dots, K\}$ ,  $\alpha^0 = \Theta$  (very large),  $\rho^0 = \epsilon$  (very small)

$\xi^0$ : random but compliant with C6

% Do the admission control

1 Solve (8) according to Algorithm 3, set  $\xi^0 = \xi^{\text{ini}}$ ,  $\rho^0 = \rho^{\text{ini}}$ ,  $v^0 = v^{\text{ini}}$ , and return  $\mathcal{K}^*$

% Optimize the allocated resources for cost minimization

2 Solve (7) according to Algorithm 4

**Output:**  $\xi^*$ ,  $\rho^*$ ,  $v^*$

---

DPATO, we decouple the power allocation from the task offloading optimization. The power allocation and task offloading optimization problems are similar to [8] and [4], respectively. Thus, the power allocation subproblem is solved first, and then we deal with the task offloading subproblem. We assume that the radio part of the network has no information about the network graph and resources therein and vice-versa, a common assumption by previous works [4]. Moreover, we should assume that the maximum tolerable latency of tasks is divided into two parts:  $T_k^{\text{RAN}}$  and  $T_k - T_k^{\text{RAN}}$ , where  $T_k^{\text{RAN}}$  is the part which is satisfied in radio domain and  $T_k - T_k^{\text{RAN}}$  is satisfied in the network graph. Thus, the convexified version of the power allocation subproblem for the disjoint algorithm is given by

$$\begin{aligned} \min_{\rho} \quad & \sum_{k \in \mathcal{K}} \rho_k \\ \text{s.t.} \quad & \text{C1-d: } h_k(\rho) - \hat{g}_k(\rho) \geq \frac{D_k}{T_k^{\text{RAN}}}, \quad \forall k \in \mathcal{K} \\ & \text{C4-a, C5.} \end{aligned} \quad (25)$$

Again, we need an admission control mechanism to ensure the feasibility of this problem. Like the joint optimization problem, we adopt the elasticization approach. Therefore, the elasticized version of (25) can be stated as

$$\begin{aligned} \min_{\rho} \quad & \sum_{k \in \mathcal{K}} \nabla T_k^{\text{tx}}(\rho^0)^{\text{T}} (\rho - \rho^0) \\ \text{s.t.} \quad & \text{C1-e: } h_k(\rho) - \hat{g}_k(\rho) \geq \frac{D_k}{T_k^{\text{RAN}} + \alpha_k}, \quad \forall k \in \mathcal{K} \\ & \text{C4-a, C5.} \end{aligned} \quad (26)$$

which is solved via CCP. After the solution of (26), the elastic variables are updated as  $\alpha_k = [T_k^{\text{tx}} - T_k^{\text{RAN}}]^+$  and then the task with maximum elastic variable is eliminated. This procedure is repeated until a feasible subset of tasks for power allocation obtained. After this step, subproblem (25) is solved according to the feasible subset of tasks. The disjoint admission control and power allocation method is shown in Algorithm 6. Given the power allocation solution, we solve the

---

**Algorithm 6:** Admission control and power allocation algorithm for disjoint method for solving (25) and (26)

---

**Input:**  $\mathcal{K} = \{1, \dots, K\}, i = 0, \alpha^0 = \Theta$  (very large),  $\rho^0 = \epsilon$  (very small),

$$T_k^{\text{RAN}} = (0, T_k), \forall k \in \mathcal{K}$$

1 **repeat**

2     **repeat**

    % Allocate power to the users to minimize the sum of the transmission latencies

3     Solve (26) via CCP in Algorithm 1 and set  $\rho^{i+1} = \rho^*$

    % Update the elastic variables

4      $s_k^{i+1} = [T_k^{\text{RAN}} - T_k^{\text{tx}}]^+, \quad \forall k \in \mathcal{K}$

5      $i = i + 1$

6     **until**  $\sum_{k \in \mathcal{K}} \alpha_k^{i-1} - \sum_{k \in \mathcal{K}} \alpha_k^i \leq \epsilon$  *or*  $i \geq I_{\max}$

    % Find the task with maximum associated elastic variable

7      $k^* = \arg \max_{k \in \mathcal{K}} \alpha_k^i$

8     **if**  $\alpha_{k^*} > 0$  **then**

    % Eliminate the task with maximum associated elastic variable

9      $\mathcal{K} = \mathcal{K} \setminus \{k^*\}$

10    **else**

11    **break**

12 **until**  $\sum_{k \in \mathcal{K}} \alpha_k = 0$

    % Allocate power to the users with the cost minimization objective

13 Solve (25) via CCP in Algorithm 1 and return  $\rho^*$

**Output:**  $\rho^*, \mathcal{K}^{\text{RAN}}$

---

task offloading subproblem. The task offloading subproblem of disjoint algorithm is split into computational resource allocation and task placement steps. More formally, we have

$$\begin{aligned} \min_{\mathbf{v}} \quad & \sum_{n \in \mathcal{N}} \sum_{k \in \mathcal{K}} \sum_{b \in \mathcal{B}_n} \Lambda_n \xi_{p_n^b}^k v_k^3 \\ \text{s.t.} \quad & \text{C1-f: } T_k^{\text{prop}} + \frac{L_k}{v_k} \leq T_k - T_k^{\text{RAN}}, \quad \forall k \in \mathcal{K}, \\ & \text{C2,} \end{aligned} \tag{27}$$

and

$$\begin{aligned} \min_{\xi} \quad & \sum_{k \in \mathcal{K}} T_k^{\text{prop}} \\ \text{s.t.} \quad & \text{C1-f, C2, C3.} \end{aligned} \tag{28}$$

Similar to the power allocation algorithm, we need an admission control mechanism for the task offloading subproblem which can be achieved by elasticization. The elasticized versions of subproblems (27) and (28) are as follows:

$$\begin{aligned} \min_{\mathbf{v}} \quad & \sum_{k \in \mathcal{K}} T_k^{\text{exe}} \\ \text{s.t.} \quad & \text{C1-g: } T_k^{\text{prop}} + \frac{L_k}{v_k} \leq T_k - T_k^{\text{RAN}} + \alpha_k, \quad \forall k \in \mathcal{K} \\ & \text{C2,} \end{aligned} \quad (29)$$

and

$$\begin{aligned} \min_{\xi} \quad & \sum_{k \in \mathcal{K}} T_k^{\text{prop}} \\ \text{s.t.} \quad & \text{C1-g: } T_k^{\text{prop}} \leq T_k - T_k^{\text{RAN}} + \alpha_k - T_k^{\text{exe}}, \quad \forall k \\ & \text{C2, C3, C6.} \end{aligned} \quad (30)$$

When the solutions of (29) and (30) are obtained, the elastic variables are updated by  $\alpha_k = [T_k^{\text{exe}} + T_k^{\text{prop}} - T_k + T_k^{\text{RAN}}]^+$  and the algorithm continues until a feasible subset of constraints is achieved. The disjoint admission control and task offloading is shown in Algorithm 7.

## VII. COMPUTATIONAL COMPLEXITY

In this section, we analyze the computational complexity of the proposed algorithms. The computational complexity of JPATO admission control algorithm is derived from the computational complexity of solving the four subproblems and the computational complexity of the ASM modification algorithm. We adopt CVX solver for solving these subproblems in order to exploit IPM for finding the optimal solution [27]. Based on [28] and [29], the required number of iterations for IPM converge is given by  $\frac{\log N_c}{\log \frac{t^0 \varrho}{\log \varsigma}}$  where  $N_c$  is the total number of constraints,  $t^0$  is the initial point for approximation of the barrier function,  $\varrho$  is the desired accuracy of convergence and  $0 < \varsigma \ll 1$  is used for updating the stepsize of the barrier function accuracy. Therefore, the computational complexity of subproblems can be given as in Table IIa. It is important to note that since we adopt CCP for solving the power allocation subproblem, we need to multiply the computational complexity of solving (18) by maximum permitted iterations of CCP, i.e.,  $I_{\max}^p$ . Additionally, Algorithm 2 puts further computational complexity on admission control algorithm. The required computations for calculation of the parameters in Algorithm 2 are provided in Table IIb where  $B$  is the maximum number of the paths between any node and  $\bar{n}$  whereas  $E$  is the total number of the edges in the network graph  $G$ . Hence, the overall computational complexity of Algorithm 2 is  $\mathcal{O}(K^2 \times N \times B \times E)$ . The computational complexity of the admission control

---

**Algorithm 7:** Admission control and task offloading algorithm of disjoint method for solving (27) - (30)

---

**Input:**  $\mathcal{K}^{\text{RAN}}$ ,  $i = 0$ ,  $\alpha^0 = \Theta$  (very large),  $\xi^0$ : random but compliant with C6

---

```

1 repeat
2   repeat
3     % Allocate computational resources to the tasks
4     Solve (29) and set  $\mathbf{v}^{i+1} = \mathbf{v}^*$ 
5     % Determine the node and the path for offloading the tasks
6     Solve (30) and set  $\xi^{i+1} = \xi^*$ 
7     % Update the elastic variables
8      $\alpha_k^{i+1} = [T_k - T_k^{\text{RAN}} - T_k^{\text{exe}} - T_k^{\text{prop}}]^+$ 
9     Update  $\mathbf{v}^{i+1}$ ,  $\xi^{i+1}$  and  $\alpha^{i+1}$  via the ASM modification algorithm (Algorithm 2)
10     $i = i + 1$ 
11  until  $\sum_{k \in \mathcal{K}} \alpha_k^{i-1} - \sum_{k \in \mathcal{K}} \alpha_k^i \leq \epsilon$  or  $i \geq I_{\max}$ 
12  % Find the task with maximum associated elastic variable
13   $k^* = \arg \max_{k \in \mathcal{K}} \alpha_k$ 
14  if  $\alpha_{k^*} > 0$  then
15    % Eliminate the task with maximum associated elastic variable
16     $\mathcal{K} = \mathcal{K} \setminus \{k^*\}$ 
17  else
18    break
19 until  $\sum_{k \in \mathcal{K}} \alpha_k = 0$ 
20 Set  $i = 0$ 
21 repeat
22   % Allocate computational resources to the tasks with the cost minimization objective
23   Solve (27) and set  $\mathbf{v}^{i+1} = \mathbf{v}^*$ 
24   % Determine the node and the path for offloading the tasks with the cost minimization
25   objective
26   Solve (28) and set  $\xi^{i+1} = \xi^*$ 
27 until  $\Psi(\xi^{i-1}, \mathbf{v}^{i-1}, \rho^*) - \Psi(\xi^i, \mathbf{v}^i, \rho^*) \leq \epsilon$  or  $i \geq I_{\max}$ 

```

**Output:**  $\xi^*$ ,  $\rho^*$ ,  $\mathbf{v}^*$ ,  $\mathcal{K}^{\text{Disjoint}}$

---

TABLE II: Computational complexity of solving different subproblems

(a) The computational complexity of subproblems		(b) The computational complexity of parameters involved in the ASM modification algorithm	
Subproblems	Complexity	Parameter	Computational Complexity
Computational resource allocation (11)	$\frac{\log(2K+N)}{t^0 \varrho \log \varsigma}$	$\mathcal{N}^k$	$N \times E$
Power allocation (18)	$\frac{\log(2K+U+E)}{t^0 \varrho \log \varsigma}$	$\tilde{\Upsilon}_n^k$	$B \times (K - 1)$
Task placement (19)	$\frac{\log(N+B+K)}{t^0 \varrho \log \varsigma}$	$\tilde{B}_{(m,m')}^k$	$N \times B \times (K - 1)$
		$(n^*, b^*)$	$N \times B$

algorithm can be obtained by aggregating the computational complexity of all subproblems and Algorithm 2. More formally, we have

$$CC^{AC} = K \times I_{\max} \left( \frac{\log(2K+N)}{t^0 \varrho \log \varsigma} + I_{\max}^{\rho} \times \frac{\log(2K+U+E)}{t^0 \varrho \log \varsigma} + \frac{\log(N+B+K)}{t^0 \varrho \log \varsigma} + \mathcal{O}(K^2 N B E) \right). \quad (31)$$

Similarly, the computational complexity of JPATO algorithm can be obtained as

$$CC^{JPATO} = I_{\max} \left( \frac{\log(2K+N)}{t^0 \varrho \log \varsigma} + I_{\max}^{\rho} \times \frac{\log(2K+U+E)}{t^0 \varrho \log \varsigma} + \frac{\log(N+B+K)}{t^0 \varrho \log \varsigma} \right). \quad (32)$$

## VIII. SIMULATION RESULTS

In this section, we evaluate the performance of the JPATO and DPATO for admission control as well as joint task offloading and power allocation. The setup of our simulation is presented in Table III. We assume that  $U = 4$  RRHs are placed with inter site distance of 100 m and all users are served in an area of 100 m radius with a given user-RRH assignment. The network graph consists of  $N = 6$  nodes at three different tiers:  $\bar{n}$  at the local tier with zero propagation delay, three nodes in the regional tier with relatively low propagation delay and two distant nodes at the national tier. For simplicity of comparison, we assume that all nodes have equal computational capacity and all tasks have equal size, load, and maximum tolerable latency. Moreover, we assume equal propagation delay and bandwidth for the network links. Note that the relatively low value of link bandwidth (0.4 Gbps) is the amount of bandwidth solely reserved to MEC tasks. Fig. 3a reports the performance of admission control algorithm in JPATO, showing the acceptance ratio versus maximum tolerable latency of tasks. More in depth, the acceptance ratio is defined as the ratio of accepted services by the admission control algorithm over the total number of the requested tasks. By observing the figure, we can note that the acceptance ratio increases by increasing the maximum tolerable latency of tasks. This is due to the fact that the tasks with higher maximum tolerable latency need less resources (transmit power and computation) in

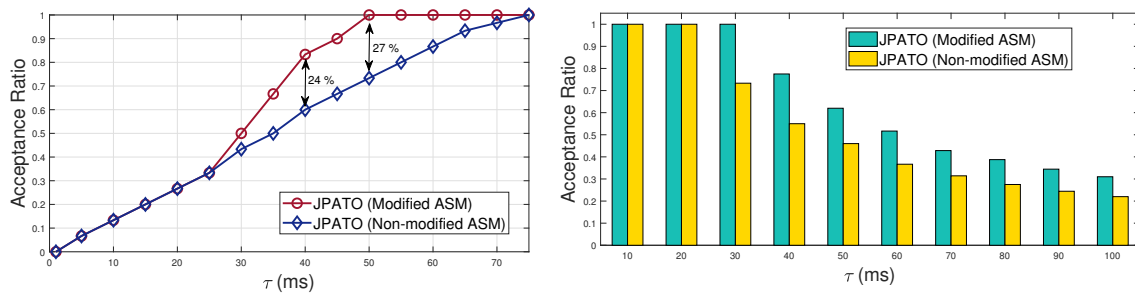


TABLE III: Simulation Setup

Parameter	Value	Parameter	Value
$L_k$	$10^6$ CPU Cycles	$\delta_{(m,m')}$	10 ms
$M$	32 Antennas	$\gamma_{(m,m')}$	$10^{-8}$ per bps
$D_k$	0.1 Mbits	Path Loss	$128.1 + 37.6 \log Q$ [8]
$\Upsilon_n$	$10^9$ CPU Cycles per Second [7]	$U$	4
$P_k^{\max}$	0.5 Watt	ISD	100 m
$B_{(m,m')}$	0.4 Gbps	$W$	20 MHz [8]
$B_{f,u}$	0.6 Gbps	Noise power	-150 dBm/Hz [8]
$\Lambda_n$	$10^{-28}$ [23]		

order to be served. Moreover, for higher maximum tolerable latencies, there are more available nodes for tasks that can be offloaded. On the other hand, the effectiveness of the Algorithm 2 can be seen in Fig. 3a, as for latencies smaller than 75 ms, outperforms the non-modified ASM algorithm. Moreover, the performance of the two methods is identical for low values of  $T$ . This is due to the fact that the set of accessible NFV-enabled nodes for low values of maximum tolerable latencies is restricted to  $\bar{n}$  and therefore, the modified ASM cannot offload the tasks to more distant NFV-enabled nodes because the corresponding propagation delay would tolerate the maximum tolerable latency of tasks.

The acceptance ratio of the JPATO admission control algorithm for different number of tasks is shown in Fig. 3b. Since the amount of available resources is limited, the acceptance ratio is decreasing with increase in the total number of users. Again, the superiority of modified ASM over non-modified ASM can be observed.



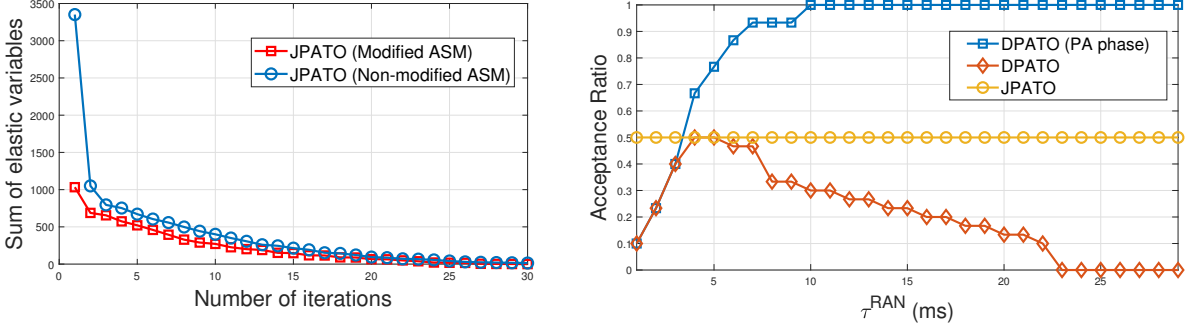
(a) The acceptance ratio vs. maximum tolerable latency for  $K = 30$ .

(b) The acceptance ratio vs. total number of tasks  $T = 40$  ms.

Fig. 3: The variations of acceptance ratio vs. maximum tolerable latency and number of tasks

The convergence of the JPATO admission control algorithm is shown in Fig. 4a. As it is proven,

the sum of elasticization variables is decreasing in each iteration. Furthermore, it is shown that the convergence of the modified ASM algorithm is faster than non-modified ASM algorithm which stems from higher acceptance ratio of modified ASM algorithm. The performance of the JPATO

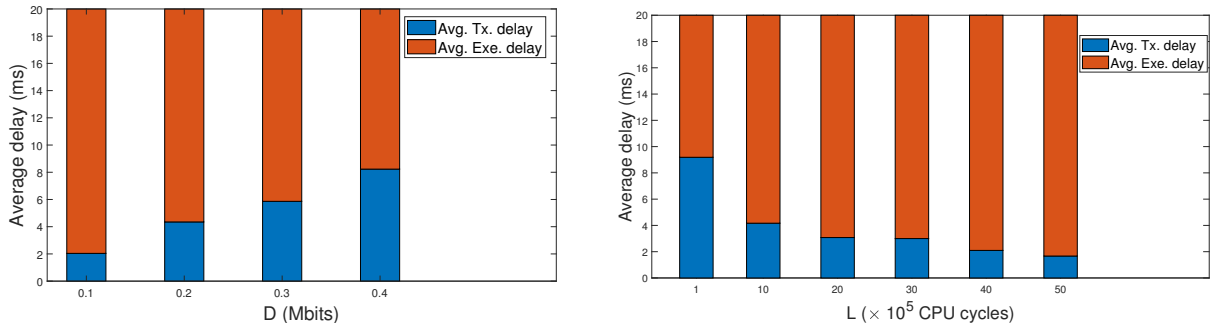


(a) The convergence of admission control algorithm for  $T = 20$  ms and  $K = 30$ .

(b) The acceptance ratio of joint vs. disjoint methods in terms of  $T^{\text{RAN}}$  for  $T = 30$  ms and  $K = 30$  users

Fig. 4: Performance of the proposed methods in terms of convergence and acceptance ratio

can be compared with DPATO based on acceptance ratio criterion. In Fig. 4b, the acceptance ratio of the JPATO and the DPATO is depicted for the tasks with maximum tolerable latency of  $T = T_k = 30$  ms. For the disjoint method, we obtain the acceptance ratio for different values of  $T^{\text{RAN}} \in (0, T)$ . Moreover, the acceptance ratio of admission control and power allocation algorithm is depicted. As it is shown in the figure, the acceptance ratio of the disjoint method is increasing for small values of  $T^{\text{RAN}}$ , that is, the small values of  $T^{\text{RAN}}$  impose high rates on users which can not be realized due to either interference or limited fronthaul capacity. On the other hand, for larger values of  $T^{\text{RAN}}$ , the acceptance ratio of the admission control and power allocation algorithm is 1 but the task offloading algorithm restricts the number of accepted tasks. Furthermore, it can be observed that the joint method outperforms the disjoint method for different values of  $T^{\text{RAN}}$ . Fig. 5a shows the average transmission delay of radio access network i.e.,  $\frac{1}{|\mathcal{K}|} \sum_{k \in \mathcal{K}} T_k^{\text{tx}}$  and the average execution delay of tasks, i.e.,  $\frac{1}{|\mathcal{K}|} \sum_{k \in \mathcal{K}} T_k^{\text{exe}}$  for different values of data size of tasks  $D = D_k, \forall k$  and maximum tolerable latency  $T = 20$  ms. As it can be observed, the average transmission delay increases by increasing the value of  $D$ , however, the average execution delay is decreased to maintain the maximum tolerable latency. Therefore, we can infer that the JPATO efficiently manages the radio resources and the computational resources for a successful task offloading. Similarly, the execution time of tasks increases by increasing



(a) The average delay of tasks transmission and execution delays in terms of data size  $D$  for  $T = 20$  ms and  $K = 30$  (b) The average delay of tasks transmission and execution delays in terms of tasks load  $L$  for  $T = 20$  ms and  $K = 30$

Fig. 5: The average delay of tasks transmission and execution delays using JPATO

the load of tasks. However, this increase can be compensated by lower transmission delay of the wireless link. Fig. 5b shows the average transmission delay of the radio access network and the average execution delay of tasks for different values of tasks loads  $L = L_k, \forall k$  and maximum tolerable latency  $T = 20$  ms. In order to evaluate the performance of the JPATO, we assume there are three classes of tasks (each class consists of 10 tasks) with three different maximum tolerable latencies, i.e.,  $T^{(1)} = 10$  ms,  $T^{(2)} = 50$  ms, and  $T^{(3)} = 100$  ms. The classes (1), (2), and (3) are considered as the sets of tasks with low, medium, and high latency requirement, respectively. Moreover, we assume there are three nodes (shown by rectangles in Fig. 6) with three different propagation delays, i.e., a local node (i.e.,  $\bar{n}$ ) with zero propagation delay, a regional node with 20 ms propagation delay, and a national node with 40 ms propagation delay. The propagation delays are assumed two-way, i.e., uplink+downlink propagation delays. Fig. 6 shows the task placement for different values of computational capacity of nodes  $C = \Upsilon_n, \forall n$ . As it is illustrated by Fig. 6, the nodes are not capable of serving class (1) of tasks due to their high resource utilization for  $C = 1$ , however, other two classes are served such that the tasks in class (2) are mainly served at local node and class (3) tasks are placed at regional and national node. By increasing the computational capacity to  $C = 10$ , some of the tasks in class (1) are placed at the local node. Moreover, some tasks in class (2) and (3) can be served at the local node as well. Furthermore, the national node does not serve any task because the JPATO tries to place the tasks at the nearest nodes in order to reduce the power consumption in the radio access network. When the computational capacity increases to  $C = 20$ , we observe that more tasks of class (1) are served at the local node and the acceptance ratio reaches to 1. By increasing even

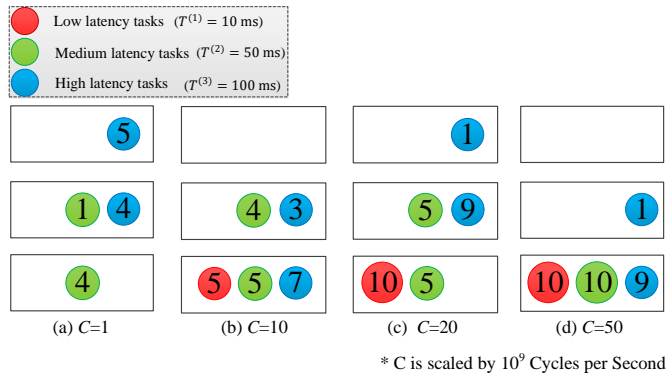


Fig. 6: The placement of the different classes of tasks at three different tiers of nodes for  $K = 30$ .

more the computational capacity to  $C = 50$ , almost all of tasks are placed at the local node in order to reduce the power consumption in the radio access network.

Table IV shows the acceptance ratio of each class for different values of computational capacity of nodes. It can be found out that the acceptance ratio of all classes is increased by increasing the computational capacity of nodes. Moreover, the acceptance ratio of class (1) is lower than that of classes (2) and (3). The reason is twofold, one is due to high resource utilization by tasks of this class and another is due to limited number of available nodes for tasks with low latency requirement (only node  $\bar{n}$  in this example).

TABLE IV: The acceptance ratio of JPATO for different task classes w.r.t. computational capacity of nodes

Computational capacity ( $10^9$ CPU cycles/sec)	Maximum tolerable latency (ms)		
	$T^{(1)} = 10$	$T^{(2)} = 50$	$T^{(3)} = 100$
$C = 1$	0	0.5	0.9
$C = 10$	0.5	0.9	1
$C = 20$	1	1	1
$C = 50$	1	1	1

## IX. CONCLUSION

In this paper, we considered a task offloading problem in a cost-efficient manner while each task was constrained to a maximum tolerable latency. We investigated the joint impact of radio transmission, propagation of tasks through the transport network, and execution of tasks on the

experienced latency of tasks. Due to the non-convexity of the optimization problem, we adopted the ASM which turned the optimization problem into: power allocation, task placement, and computational resource allocation subproblems. The power allocation was solved by adopting CCP to convexify the subproblem. The task placement and computational resource allocation were modeled as an ILP and convex subproblem, respectively. Moreover, we proposed a heuristic method based on ASM, with the goal of placing the tasks in more distant nodes when the computational resources are sufficient. Furthermore, to ensure the feasibility of optimization problem, we proposed an admission control mechanism to eliminate the tasks causing infeasibility. On the other hand, we proposed a disjoint optimization method as our baseline of comparison in which, the optimization problem was cut down into two parts, one for radio transmission and one for task placement and computational resource allocation. The simulation results showed the superiority of JPATO w.r.t. DPATO. The performance of the disjoint method depended on the part of latency required to be met in radio access network, i.e.,  $T^{\text{RAN}}$ . However, the joint method showed higher acceptance ratio for different values of  $T^{\text{RAN}}$ . Incorporating the task scheduling into JPATO can be regarded as a future line of research. Moreover, dividing the required computational load of the tasks into several nodes and merging the results is a worth investigating problem for future research.

## REFERENCES

- [1] B. Yi, X. Wang, K. Li, S. K. Das, and M. Huang, "A comprehensive survey of network function virtualization," *Computer Networks*, vol. 133, pp. 212–262, 2018.
- [2] P. Mach and Z. Becvar, "Mobile edge computing: A survey on architecture and computation offloading," *IEEE Communications Surveys & Tutorials*, vol. 19, no. 3, pp. 1628–1656, 2017.
- [3] ETSI, "Mobile Edge Computing (MEC); Framework and reference architecture," *ETSI Group Specification MEC 003*, 2016.
- [4] B. Yang, W. K. Chai, Z. Xu, K. V. Katsaros, and G. Pavlou, "Cost-efficient NFV-enabled mobile edge-cloud for low latency mobile applications," *IEEE Transactions on Network and Service Management*, vol. 15, no. 1, pp. 475–488, 2018.
- [5] T. Li, C. S. Magurawalage, K. Wang, K. Xu, K. Yang, and H. Wang, "On efficient offloading control in cloud radio access network with mobile edge computing," in *2017 IEEE 37th International Conference on Distributed Computing Systems (ICDCS)*, pp. 2258–2263, IEEE, 2017.
- [6] H. Guo, J. Liu, and J. Zhang, "Computation offloading for multi-access mobile edge computing in ultra-dense networks," *IEEE Communications Magazine*, vol. 56, no. 8, pp. 14–19, 2018.
- [7] L. Yang, H. Zhang, M. Li, J. Guo, and H. Ji, "Mobile edge computing empowered energy efficient task offloading in 5G," *IEEE Transactions on Vehicular Technology*, vol. 67, no. 7, pp. 6398–6409, 2018.
- [8] W. Xia, J. Zhang, T. Q. Quek, S. Jin, and H. Zhu, "Power minimization-based joint task scheduling and resource allocation in downlink C-RAN," *IEEE Transactions on Wireless Communications*, vol. 17, no. 11, pp. 7268–7280, 2018.

- [9] J. Zhang, W. Xia, F. Yan, and L. Shen, "Joint computation offloading and resource allocation optimization in heterogeneous networks with mobile edge computing," *IEEE Access*, vol. 6, pp. 19324–19337, 2018.
- [10] J. G. Herrera and J. F. Botero, "Resource allocation in NFV: A comprehensive survey," *IEEE Transactions on Network and Service Management*, vol. 13, no. 3, pp. 518–532, 2016.
- [11] M. M. Tajiki, S. Salsano, L. Chiaraviglio, M. Shojafar, and B. Akbari, "Joint energy efficient and QoS-aware path allocation and VNF placement for service function chaining," *IEEE Transactions on Network and Service Management*, vol. 16, no. 1, pp. 374–388, 2019.
- [12] T. X. Tran and D. Pompili, "Joint task offloading and resource allocation for multi-server mobile-edge computing networks," *IEEE Transactions on Vehicular Technology*, vol. 68, no. 1, pp. 856–868, 2019.
- [13] J. Li, H. Gao, T. Lv, and Y. Lu, "Deep reinforcement learning based computation offloading and resource allocation for MEC," in *2018 IEEE Wireless Communications and Networking Conference (WCNC)*, pp. 1–6, IEEE, 2018.
- [14] M.-H. Chen, M. Dong, and B. Liang, "Resource sharing of a computing access point for multi-user mobile cloud offloading with delay constraints," *IEEE Transactions on Mobile Computing*, vol. 17, no. 12, pp. 2868–2881, 2018.
- [15] W. Almughalles, R. Chai, J. Lin, and A. Zubair, "Task execution latency minimization-based joint computation offloading and cell selection for MEC-enabled HetNets," in *2019 28th Wireless and Optical Communications Conference (WOCC)*, pp. 1–5, IEEE, 2019.
- [16] M. A. T. Nejad, S. Parsaeefard, M. A. Maddah-Ali, T. Mahmoodi, and B. H. Khalaj, "vSPACE: VNF simultaneous placement, admission control and embedding," *IEEE Journal on Selected Areas in Communications*, vol. 36, no. 3, pp. 542–557, 2018.
- [17] S. Li, N. Zhang, S. Lin, L. Kong, A. Katangur, M. K. Khan, M. Ni, and G. Zhu, "Joint admission control and resource allocation in edge computing for internet of things," *IEEE Network*, vol. 32, no. 1, pp. 72–79, 2018.
- [18] V. Eramo, E. Miucci, M. Ammar, and F. G. Lavacca, "An approach for service function chain routing and virtual function network instance migration in network function virtualization architectures," *IEEE/ACM Transactions on Networking*, vol. 25, no. 4, pp. 2008–2025, 2017.
- [19] Q.-V. Pham, F. Fang, V. N. Ha, M. Le, Z. Ding, L. B. Le, and W.-J. Hwang, "A survey of multi-access edge computing in 5G and beyond: Fundamentals, technology integration, and state-of-the-art," *arXiv preprint arXiv:1906.08452*, 2019.
- [20] A. Khalili, S. Zarandi, and M. Rasti, "Joint resource allocation and offloading decision in mobile edge computing," *IEEE Communications Letters*, vol. 23, no. 4, pp. 684–687, 2019.
- [21] X. Chen, L. Jiao, W. Li, and X. Fu, "Efficient multi-user computation offloading for mobile-edge cloud computing," *IEEE/ACM Transactions on Networking*, vol. 24, no. 5, pp. 2795–2808, 2015.
- [22] K. Zhang, Y. Mao, S. Leng, Q. Zhao, L. Li, X. Peng, L. Pan, S. Maharjan, and Y. Zhang, "Energy-efficient offloading for mobile edge computing in 5G heterogeneous networks," *IEEE access*, vol. 4, pp. 5896–5907, 2016.
- [23] F. Zhou, Y. Wu, R. Q. Hu, and Y. Qian, "Computation rate maximization in UAV-enabled wireless-powered mobile-edge computing systems," *IEEE Journal on Selected Areas in Communications*, vol. 36, no. 9, pp. 1927–1941, 2018.
- [24] J. W. Chinneck, *Feasibility and Infeasibility in Optimization*. Algorithms and Computational Methods, Springer, 2008.
- [25] T. Lipp and S. Boyd, "Variations and extension of the convexconcave procedure," *Optimization and Engineering*, vol. 17, no. 4, pp. 263–287, 2016.
- [26] MOSEK ApS, *The MOSEK optimization toolbox for MATLAB manual. Version 9.0.*, 2019.
- [27] CVX Research, Inc., "CVX: Matlab software for disciplined convex programming, version 2.0." <http://cvxr.com/cvx>, 2012.
- [28] N. Mokari, F. Alavi, S. Parsaeefard, and T. Le-Ngoc, "Limited-feedback resource allocation in heterogeneous cellular networks," *IEEE Transactions on Vehicular Technology*, vol. 65, pp. 2509–2521, April 2016.
- [29] S. Boyd and L. Vandenberghe, *Convex Optimization*. New York, NY, USA: Cambridge University Press, 2004.